Preferred citation: A. Ketola, T. Hjelt, T. Lappalainen, H. Pajari, T. Tammelin, K. Salminen, K.Y. Lee, O. Rojas and J.A. Ketoja. The relation between bubble-fibre interaction and material properties in foam forming. In *Advances in Pulp and Paper Research*, Cambridge 2022, Trans. of the XVIIth Fund. Res. Symp. Cambridge, 2022 (D. Coffin and W. Batchelor, eds), pp 65–84. FRC, Manchester, 2022. DOI: 10.15376/frc.2022.1.65.

THE RELATION BETWEEN BUBBLE-FIBRE INTERACTION AND MATERIAL PROPERTIES IN FOAM FORMING

Annika Ketola[1,], Tuomo Hjelt[1], Timo Lappalainen[1], Heikki Pajari[1], Tekla Tammelin[1], Kristian Salminen[1], Koon-Yang Lee[2], Orlando Rojas[3] and Jukka A. Ketoja[1]*

[1] VTT Technical Research Centre of Finland Ltd, P.O. Box 1603, FI-40101 Jyväskylä, Finland

[2] Department of Aeronautics, Imperial College London, City and Guilds Building, SW7 2AZ, London, UK

[3] Bioproducts Institute, Departments of Chemical & Biological Engineering, Chemistry and Wood Science, The University of British Columbia, 2360 East Mall, Vancouver, BC V6T 1Z3, Canada

ABSTRACT

Foam forming of cellulose fibre materials is based on an interaction between fibres and bubbles, which can take several material properties to new levels. To control the formed structure, the mechanisms of this interaction have been systematically investigated. This started with captive bubble studies where we analysed the interaction of a single bubble with various smooth cellulose and silica model surfaces. The bubbles adhered only to hydrophobic surfaces, and this attraction was sensitive to the surface tension. From this simplest case, the studied system gradually became more complex. We found that a bubble adheres weakly also to a submerged cellulose nanofibre (CNF) film, which could be explained by nanoscale surface roughness capturing nanobubbles. The interaction with real fibres was

* Corresponding annika.ketola@vtt.fi

studied by pressing a single bubble against a fibre bed in water and sodium dodecyl sulphate (SDS) solution. Fibre type and surface tension had all apparent effects on the attachment. In the case of natural fibres, the presence of hydrophobic lignin clearly increased the fibre attachment on a bubble, while added SDS decreased the attachment with all fibre types. These findings agreed with the mechanisms found earlier using the model surfaces. Finally, when forming thick nonwoven materials using hydrophilic and hydrophobic viscose fibres, differences in fibre network structure and strength properties depended on the fibre hydrophobicity and surfactant type, as suggested by the results obtained in simpler systems.

INTRODUCTION

The climate crisis, overuse of natural resources and loss of biodiversity have awakened both consumers and policy-makers [1]. The resulting actions toward the circular economy have forced many industry sectors to change their current operation models. Recyclable and renewable biomaterials are under extensive research, and cellulose, being one of the most abundant biopolymers on earth, has drawn a lot of attention. The paper and board industry has used cellulose fibres for decades, but the fast technological development has decreased the demand for paper. At the same time, new opportunities for cellulose products arise, partly because of the intriguing inherent properties of cellulose fibres, and partly because of the need to replace disposable plastics in certain product areas.

Expanding the use of fibre materials requires versatile production technologies, such as foam forming introduced already in the 1960s by Radvan et al. [2]–[4]. Wet foam is an excellent carrier media for challenging raw materials such as lightweight nanoparticles, long textile fibres or complex material combinations. In wet foam, fibres arrange themselves around air bubbles [5]–[7], and after the foam removal, a self-standing porous fibre structure remains. Besides conventional thin paper sheets, the production of extremely bulky, porous and lightweight materials [8]–[10] becomes possible as the material density can be set to a new level. The potential applications include greener alternatives for packaging, air filters, insulation materials, cushioning and substrates for biocatalytic conversion.

Due to the wide application possibilities, controlling the final material properties is highly important. The density and pore size distribution of the fibre network can be affected by the stability and bubble size of the foam, surfactant

and fibre chemistry, and fibre type [7]. Thus, it is necessary to understand the interaction of bubbles with different fibre types in varied chemical environments and to link such knowledge to the architecture of the foam, its stability and rheology.

Several studies have shown bubble adhesion to fibres in foam-fibre suspensions [5]–[7], [11], but the interaction mechanisms have been unclear. The bubble-fibre interaction has been studied especially in pulp de-inking flotation, but the literature provides controversial results. Bubble-fibre interaction has been explained as being caused by hydrophobic forces between bubbles and hydrophobic lignin regions on fibre surfaces [12]. Hydrophobic interaction between bubbles and surfaces is proposed to involve surface nanobubbles that attract larger air bubbles in the solution [13]–[16]. Especially rough surfaces have pores that can trap air inside in the form of nanobubbles (radius 10–500 nm). On the other hand, others claim that the bubble-fibre interaction is mainly caused by the mechanical entrainment of fibres in the froth that moves them [17], [18]. Ajersch & Pelton [17] concluded that bubble formation on fibres would require pre-existing air on their surfaces in the form of gas pockets trapped in surface cavities (nanobubbles), and they suggested that air bubbles do not form or adhere to fully wetted fibre surfaces with a vanishing receding contact angle. However, Deng et al. [19], [20] pointed out that bubble-fibre collision in a dynamic system can overcome the zero receding contact angle and that adhesion can happen. A bubble then stays attached to the fibre surface if its advancing contact angle is greater than zero.

The variation in the surface chemistry and morphology of fibres makes the investigations of the dynamic bubble-fibre system challenging and can explain the controversial results of the different studies. In turn, bubble adhesion on better-defined solid mineral particles in froth flotation and the mechanisms behind bubble-particle interactions have been comprehensively studied in the literature [21]–[23]. Especially surface nanobubbles have been addressed as an important factor in enhancing flotation recovery [24], [25]. The existence of surface nanobubbles on hydrophobized silica and mica has been shown through the use of atomic force microscope imaging [16], [26]–[28]. Other techniques, such as infrared spectroscopy [29], different high-resolution microscopy techniques[30]–[32] and quartz crystal microbalance [33], have also been utilized to prove the presence of nanobubbles. However, direct imaging of nanobubbles on fibre surfaces in a liquid environment has not been done.

In this study, we designed a systematic approach to clarify the interaction mechanisms between wet foam and fibres in the forming process (Figure 1). The idea is to gradually increase the complexity of the studied system so that it is possible to determine chemical or physical factors that are responsible for different

interaction mechanisms. The work was begun by studying the adhesion of a single bubble to smooth silica and cellulose model surfaces with varying levels of hydrophobicity (Figure 1a). Single bubbles were shown to adhere only to hydrophobic surfaces of silica and cellulose, and this attraction was sensitive to the surface tension of the liquid phase [16]. When the contact angle of the cellulose was over 65°, the bubble formed a clear three-phase contact (TMC).

To see how nanoscale roughness, surface nanobubbles and surface amphiphilicity affect the interactions, the single bubble experiments were extended to a cellulose nanofibre (CNF) film (Figure 1a). This was followed up by captive bubble studies of immersed fibre beds (Figure 1b). Natural fibres consist mainly of cellulose, but they may also include significant amounts of lignin and hemicelluloses, depending on the fibre type and pulping process [34]. For example, lignin content of chemi-thermomechanical pulp (CTMP) fibres is around 30% [35]. Kraft pulping removes approximately 90% of the lignin so that the final lignin content is less than 5% [34]. The contact angles of single kraft and CTMP fibres have been measured to be around 30° and 45°, respectively [35], [36]. The adhesion properties found with the natural fibres were compared to smooth viscose fibres obtained from regenerated cellulose without lignin and with a contact angle in the range of 25–35° [37].

Finally, the interactions and their consequences were carefully characterised for a real laboratory forming process (Figure 1c)[38]. Interestingly, the interaction mechanisms discovered with model surfaces turned out to explain many features of the complex foam forming process.

In the current paper, we concentrate mainly on the bubble interaction with nanocellulose films and immersed fibre beds because these experiments have not been reported earlier. The cellulose nanofibre films were produced using spin-coating [39], and the bubble interaction with rough cellulose surface was studied with the captive bubble method [40] in solutions containing electrolytes and different surfactants. Anionic sodium dodecyl sulphate (SDS) and non-ionic Tween 20 were selected for these studies as they are commonly used for foam forming. Our fibre bed is a simplified version of the Automated Contact Time Apparatus (ACTA) [41], [42] consisting of a single bubble interacting with a submerged fibre bed. The studied liquids were water, degassed water and SDS solution. The degassing was performed to study indirectly the effect of surface air (or nanobubbles) on the adhesion behaviour. Direct imaging of nanobubbles with sophisticated imaging techniques was not included in this study. The included fibres were kraft pine (i.e. delignified pine), kraft birch, CTMP, and viscose (or rayon) fibres having differences in the lignin content and morphology, characterised with a scanning electron microscope (SEM) and FibreTester. The final conclusions are based on combining the obtained results with earlier discoveries made in other foam-fibre systems.

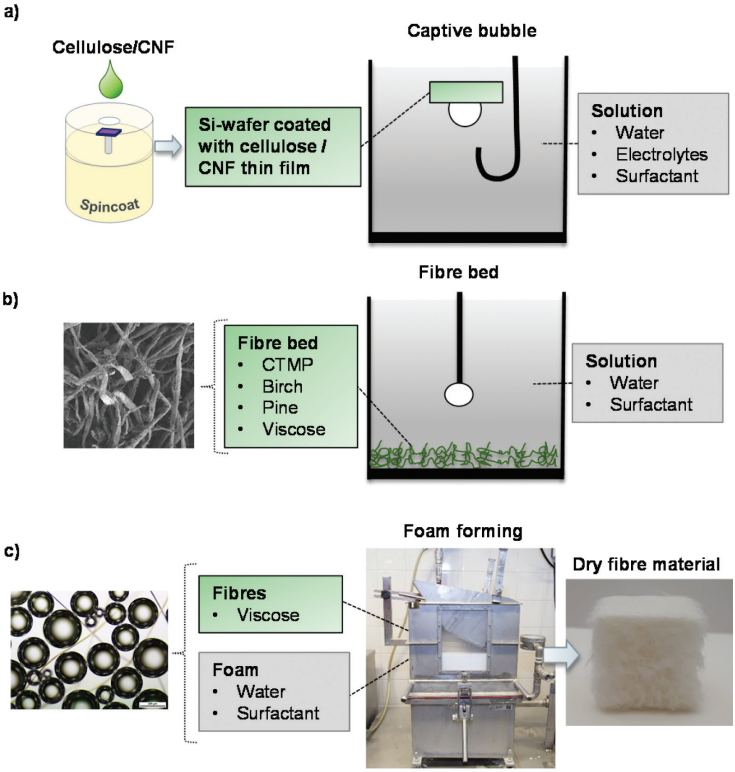

Figure 1. Systematic approach to study mechanisms of foam-fibre interaction: (a) The captive bubble method for measuring bubble attachment and adhesion to cellulose and CNF model surfaces in liquid solutions. (b) The fibre bed for measuring fibre attachment to bubbles in liquid solutions. (c) Laboratory foam-forming of bulky cellulose fibre materials. The studied material components are indicated in each case.

MATERIALS AND METHODS

All the reagents used in the experiments were of analytical grade. Anionic surfactant sodium dodecyl sulphate (SDS, purity ≥99%) and non-ionic polyethylene glycol sorbitan monolaurate (Tween 20) were purchased from Sigma-Aldrich (Germany) and were used without further purification. Sodium chloride (NaCl) was purchased from Merck (Germany). Branched Polyethylenimine (PEI) (30%, MW 50,000–100,00) was obtained from Polysciences, Inc. (United States). Water used in the experiments was Milli-Q water.

Fibre materials. Viscose fibres (Rayon 1.0 mm and 0.35 mm) were purchased from Kelheim Fibres (Germany). Pre-refined pine kraft pulp (3.7% consistency), birch kraft pulp and chemi-thermomechanical pulp (CTMP Hyper BC6100, 1.1% consistency) were provided by Metsä Board Äänekoski. CTMP was wet disintegrated before use (EN-ISO 5263–2 Part 2.). Birch kraft pulp was refined to Schopper-Riegler (SR) number 26 (3.15% consistency, KCL Espoo).

Thin films of cellulose nanofibres (CNF). Cellulose nanofibres (CNF, Masuko, 1.8% consistency) were produced from never-dried bleached birch kraft pulp. Pulp was mechanically disintegrated, and then the dispersed pulp (1.7% consistency) was pre-refined with a grinder (Supermasscolloider MKZA10-15J, Masuko Sangyo Co.) at 1500 rpm. After grinding, the pulp was fluidized (Microfluidics M-7115-30) with nine passes at an operating pressure of 1800 bar. No chemical modification was applied. A more detailed description of CNF preparation can be found in the literature [43].

Thin films of CNF were prepared according to a modified procedure previously described in the literature [39]. For spincoating, CNF was first diluted to 0.15% and ultrasonicated for 10 min at 25% amplitude (Branson 450 digital sonifier, United States) to defibrillate the material. The CNF solution was then centrifuged (Eppendorf Centrifuge 5804 R, Germany) for 45 min at 10,400 rpm, and the clear supernatant was used for the spincoating. Silica wafers (Okmetic, Espoo, Finland) were used as substrates for the CNF films. Wafers were first cleaned with UV-Ozone cleaner (Procleaner, BioForce nanosciences, USA) for 10 min and then placed in a PEI solution (0.33%) for 15 min. Wafers were washed in water to remove all the non-adsorbed material, dried with nitrogen gas and placed in a spincoater (WS-400BZ-6NPP/Lite, Laurell Technologies, USA). A few water drops were first applied onto the wafer and spun for 20 sec at 3000 rpm. Then CNF solution was applied and spun for 1.5 min at 3000 rpm. Wafers with CNF films were then heat-treated in an oven at 80°C for 10 min to attach the CNF properly to the surface.

The captive bubble method and bubble adhesion on CNF. The bubble adhesion to CNF films in different liquid environments was examined using the captive bubble method [40], [44], [45] and an optical Theta tensiometer (Attension, Biolin Scientific). The solutions used were deionised water (normal and degassed), NaCl (0.1M and 1.0M), tap water (normal and degassed), SDS (1.0, 0.3 and 0.6 g/L) and Tween 20 (6.5 g/L). The system consists of a quartz cuvette (Hellma Analytics, 20mm) containing the sample solution and a hooked needle to create the bubble. A Si wafer with CNF film was first immersed (depth about 2 mm) horizontally in the liquid, and then a bubble (volume 4 μl) was created on the head of a hooked needle placed underneath the surface (Figure 1a). The system was allowed to stabilize for 600 s while the surface tension was recorded. Then the bubble was brought into contact with the wafer (10 mm/min) and pressed against the wafer for 100 s and then removed. The removal of the bubble from the surface was

recorded. Ten replicates per test solution were conducted. The quartz cuvette and the hooked needle were carefully washed prior to and after every measurement using Deconex® and EtOH and then rinsed with water. The experiments were carried out in a controlled atmosphere of 23°C and 50% relative humidity. A more detailed description of the used captive bubble method can be found in the literature [40].

CNF hydrophobicity (contact angle measurement). An optical Theta tensiometer (Attension, Biolin Scientific) and the sessile drop method were used to measure the contact angle of water on a CNF thin film. A water drop (4 µl) was placed onto the surface, and the shape of the liquid drop was recorded. Under steady state, the surface wetting is described by Young's equation (Eq. 1)

$$\gamma_{SV} = \gamma_{SL} + \gamma_{LV} \cos\theta \quad (1)$$

where γ_{SV} is the surface free energy of the solid, γ_{SL} is the solid-liquid surface energy, γ_{LV} is the liquid surface tension and is the measured contact angle of the drop.

The fibre bed method and bubble-fibre interaction. The fibre attachment to bubbles in different liquid environments was examined using the fibre bed method, which is a simplified single bubble version of the Automated Contact Time Apparatus (ACTA) [41], [42]. Solutions used were deionised water (normal and degassed) and SDS (0.3, 0.6 and 1.0 g/L). The measurements were done using an optical Theta tensiometer (Attension, Biolin Scientific). Fibre suspension was put into a cuvette (8ml) and diluted so that a thin fibre bed was created on the bottom of the cuvette (Figure 1b). A bubble (1.0 ± 0.5 µl) was created on top of a needle and allowed to stabilize 10 min before the measurement. Then the bubble was pressed against the fibre bed for 100 s. Fifteen replicates per trial point were conducted, and the attachment probability was calculated. The experiments were carried out in a controlled atmosphere of 23 °C and 50% relative humidity.

Removal of nanobubbles by degassing. To study the effect of nanobubbles on bubble adhesion on CNF film and fibre surface, a degassing was performed. The degassed samples, including immersed CNF thin films and fibre beds in Milli-Q water and tap water were prepared using a vacuum. Sample liquids were degassed using filtering flasks and a water jet pump. A vacuum flask (25 ml in volume) was filled with water (100 ml), sealed and connected to the pump. The liquid samples were degassed for 30 min at 20 mbar vacuum so that no bubbles appeared in the liquid anymore. The CNF thin films were degassed in a similar fashion by first placing the coated wafers in a Petri dish filled with sample liquid so that the surfaces were clearly underwater. Then the Petri dish with CNF thin film was put into a desiccator with a small portion of water at the bottom to ensure a humid environment. The same method was also applied to the fibre bed samples, except that the fibres were first placed in a vacuum flask (2500 ml in volume) with dilute

fibre suspension (100 ml). After degassing as above, 10 ml of fibre suspension was ultrasonicated (20 s with 20% amplitude) to ensure the removal of any nano-bubbles. The experiments were carried out immediately after degassing.

Calcium and magnesium content of tap water. Calmagite Colorimetric Method (8030) was used to determine calcium and magnesium content of the used tap water. The calcium and magnesium content of the tap water was measured to be 24 mg/L and 1.3 mg/L, respectively.

Surface morphology and roughness. An atomic force microscope (AFM, Analys instruments, afm+) was used to determine the morphology and roughness of the CNF thin film. Silicon cantilevers (AppNano, ACTA-10, tip size <10 nm) were used in the tapping mode for scanning with a resonance frequency of 200–400 kHz. Measurements were performed in air at room temperature. The analysis studio software 3.11 was used to calculate surface roughness variation and root mean square value (RMS).

Fibre characterization with SEM and drying for imaging. Images were collected with a field-emission scanning electron microscope (FE-SEM, Zeiss Merlin, Germany) using an acceleration voltage of 2 keV and a probe current of 60 pA. The dry fibres were sputter-coated (Leica EM ACE200, Germany) with 3 nm thick Au/Pd layer prior imaging.

For imaging, the fibres were dried using critical point drying (CPD). The water in wet fibres was gradually changed to acetone by immersing the samples in water/acetone mixtures with increasing acetone concentration. Water/acetone ratios of 70/30, 50/50, 30/70, 15/85 and 5/95 were used, and the residence time in each solution was at least 10 minutes. After this, the fibres were immersed in pure acetone for 20 min, which was repeated three times. The samples in acetone were transferred to a critical point drying device (Bal-Tec CPD 030) where acetone was replaced by liquid CO_2 before drying to the critical point.

Fibre morphology. L&W FibreTester (Code 912 Plus) was used to determine the fibre geometric properties (Table 1). The measurement is based on analysing images of individual fibres in water solution.

Table 1. The fibre geometric properties were measured using the L&W FibreTester

	Mean length (mm)	*Mean width* (μm)	*Mean shape* (%)	*Mean fines* (%)	*Crill Quota* (UV/IR)	*Mean kink angle* (°)	*Number of kinks per fibre*
Pine	1.98	29.1	83	24	1.12	55	1.1
Birch SR26	0.95	21.8	91	22	0.97	50	0.4
CTMP	0.94	29.1	91	56	1.13	46	0.2
Rayon 1mm	1.01	17.4	97	1	0.81	65	0.0

RESULTS AND DISCUSSION

Bubble Adhesion to a Rough CNF film

Bubbles did not form a clear tree phase contact point with CNF films in any of the studied liquid solutions. The bubble adhesion to the needle was stronger than the adhesion to the CNF film, and the bubbles stayed attached to the needle during detachment from the film surface. However, during the detachment, bubbles elongated before fully detaching from the film, meaning that some adhesion occurred (Figure 2 a,b). Electrolytes, especially those in tap water (Ca 24 mg/L, Mg 1.3 mg/L) clearly increased the adhesion level, probably because of the charge screening effect. In contrast, with smooth cellulose film, this kind of elongation was not observed in water or in electrolyte solution [40].

The raw material of CNF was bleached birch kraft pulp so that the fibrils consisted mainly of cellulose [39]. The contact angle of the CNF film was 13° so that the surface is hydrophilic on a macroscopic scale. However, the microfibrils have amphiphilicity, which in principle could drive some nanoscale adhesive behaviour. Moreover, unlike smooth cellulose model surfaces, CNF films have some small-scale roughness (RMS 4 nm, Figure 2b). As mentioned previously, rough surfaces have pores that can trap air inside in the form of nanobubbles (radius 10–500 nm) [14], [16], [28]. Thus, besides the amphiphilicity of cellulose, the surface nanobubbles could partly explain the observed bubble attraction for CNF. This should show up as a decreasing adhesion force when the nanobubbles are removed by degassing.

The bubble adhesion indeed decreased when the whole system, including the water and the CNF film, was degassed. The effect was significant in tap water, where the bubble elongation decreased from approximately 62 μm to 12 μm. In degassed Milli-Q water, the bubble adhesion almost totally vanished. Degassing of the system was expected to decrease the amount of entrapped nanobubbles in the CNF film. The significant decrease in the bubble elongation after degassing suggests that entrapped nanobubbles have a strong impact on bubble adhesion on the CNF film. Surface roughness and uneven distribution of nanobubbles on the CNF film could also explain the high variation in the bubble elongation values.

Bubble adhesion to the CNF film in anionic SDS solutions (0.3 and 0.7 g/L) was similar to the one in deionised water, with a small elongation before detachment. The introduction of electrolytes did not change this behaviour. It is probable that surfactant adsorption on the CNF film and at air-water interfaces hindered the bubble adhesion tendency. SDS has been shown to adsorb on cellulose and CNF films already at low concentrations, but the adsorption amounts are rather small [40], [46], [47]. The surface tension of the used solutions was 63 and 51 mN/m for 0.3 and 0.7 g/L of SDS, respectively. The used concentrations of SDS seemed to be not enough to alter the bubble interaction with the surface.

However, in the nonionic Tween 20 solution, the bubble elongation increased slightly. The surface tension of the Tween 20 solution (6.5 g/L) was 36 mN/m. This low surface tension should already have had an effect on the affinity of the bubble to the CNF film because of the decreased surface energy of the bubble [20], [40]. However, non-ionic surfactants with ethoxylated surfactant headgroups have been suggested to form bridges between surfactant micelles and cellulose fibrils [48]. This bridging effect could explain the increased bubble elongation during detachment.

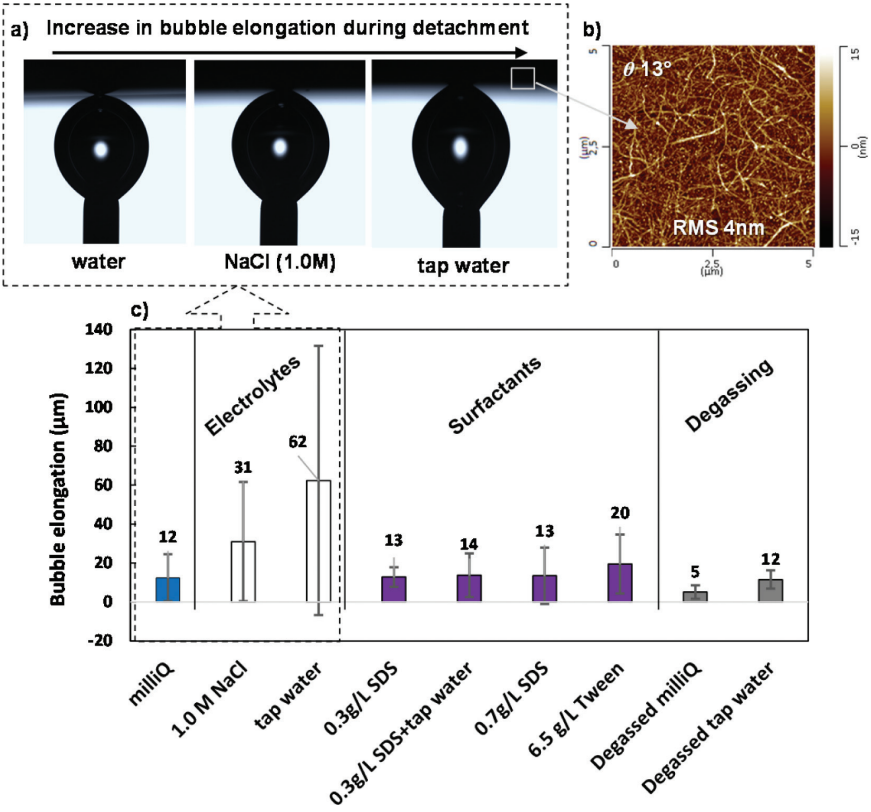

Figure 2. (a) Bubble elongation near a CNF film before detachment in water, NaCl solution and tap water (needle width 1.77mm). (b) AFM image of CNF film showing the surface roughness. (c) The effect of electrolytes, surfactants and degassing on bubble elongation behaviour for the CNF thin film during detachment. The average values with their confidence level intervals (95%) are shown.

Bubble Interaction with Cellulose Fibres

All fibre types had some affinity to bubbles in water (Figure 3). The highest attachment probability was found with light viscose fibres, and reducing their length increased the attachment probability. CTMP, with a high amount of hydrophobic lignin, had the highest attachment probability among natural fibres, while pine kraft fibres had the lowest. After degassing the system, the attachment probability decreased notably with birch and pine kraft pulps. Actually, pine did not attach at all when all air was removed. However, with CTMP and viscose fibres, the degassing increased the attachment probability. All fibres could be detached from the immersed test bubble very easily by just gently shaking the bubble in the studied solution.

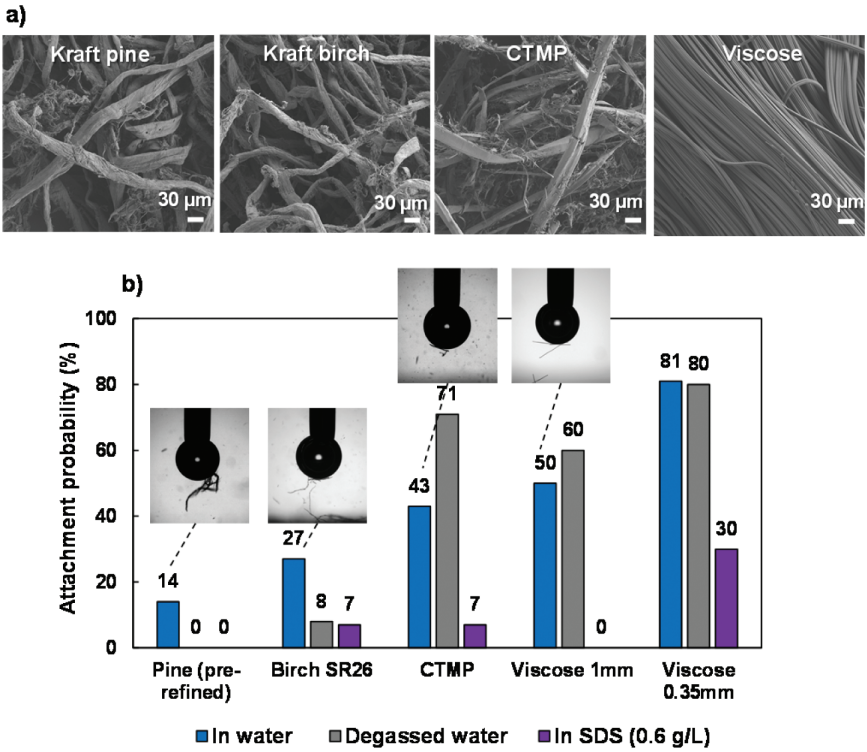

Figure 3. (a) Morphology of the different fibre types used in the measurements as imaged with SEM (200x magnification). (b) Fibre-bubble attachment probability in different environments. The bubbles were stabilized for 10 min before the experiment, and the interaction time between the bubble and the fibre bed was 100 s.

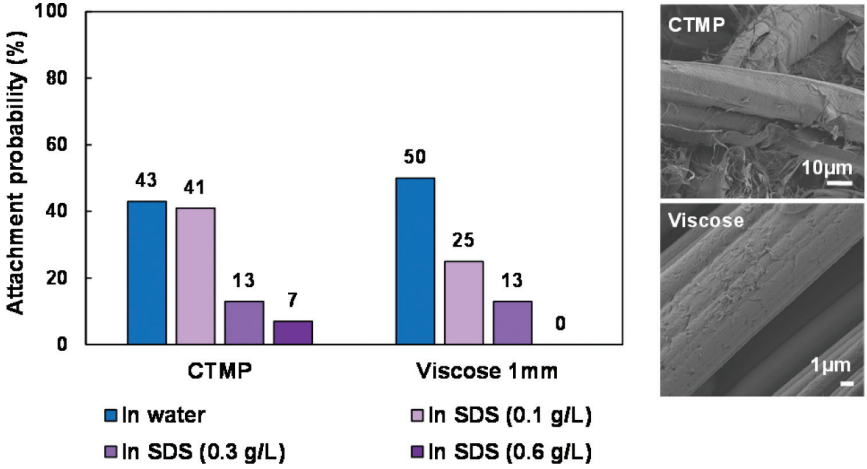

Figure 4. Attachment probability of CTMP and viscose fibres on bubbles at different SDS concentrations. Bubbles were stabilized for 10 min before the experiment, and the interaction time between the bubble and fibre bed was 100 s.

The addition of an anionic surfactant (SDS 0.6 g/L) had a significant hindering effect on the attachment for all fibre types. The effect of SDS on the bubble-fibre interaction was studied in more detail with CTMP and viscose fibres (Figure 4). Already a small addition of SDS (0.1 g/L) was able to notably decrease the bubble-viscose interaction, while there was no effect for CTMP. However, a larger amount of 0.3 g/L of SDS caused a similar effect for both fibre types, and with 0.6 g/L of SDS, the interactions almost totally vanished. It seemed that viscose fibres were slightly more sensitive to the SDS addition than CTMP at low concentrations.

According to the studies with cellulose and CNF films, natural fibres were expected to have a higher attachment probability on bubbles when compared to viscose fibres because of their rough surface with entrapped nanobubbles [17]. We expected degassing of the system to decrease the interaction as shown for the CNF film. The high interaction of smooth viscose fibres with bubbles and the increase in bubble attachment after degassing with viscose and CTMP was unexpected and controversial when compared to the results obtained using model surfaces. This discrepancy can be explained by considering both the plain interaction between a fibre and the bubble and the interaction between fibres within the bed. The attachment requires that the bubble-fibre adhesion exceeds the attachment forces arising from entanglements of fibres in the bed. Fibres have different morphologies (Table 1). Pine fibres are the longest (2mm) with the curliest struc-

ture. Viscose is the thinnest and almost entirely straight without any curl. Birch and CTMP are approximately 1 mm in length and relatively straight.

Figure 5 summarizes the mechanisms that could explain the experimental results obtained with a fibre bed. The relatively low attachment probabilities of natural fibres on bubbles compared to light viscose fibres could be explained by the larger size and curly morphology of the natural fibres and a high entanglement in the fibre bed. There might actually be less contact surface available for the bubble to interact with natural fibres than with relatively smooth viscose fibre. The interaction between a bubble and CTMP was highest among the natural fibres most likely because of the highest hydrophobic content. Bubbles have shown clear adhesion on a hydrophobic cellulose model surface with $\theta > 50°$, measured with the captive bubble method [40]. This is close to the contact angle of CTMP fibres [35], [36].

Degassing was expected to remove nanobubbles from the fibre surfaces and thus decrease the fibre attachment probability, as happened with CNF film (Figure 3.).

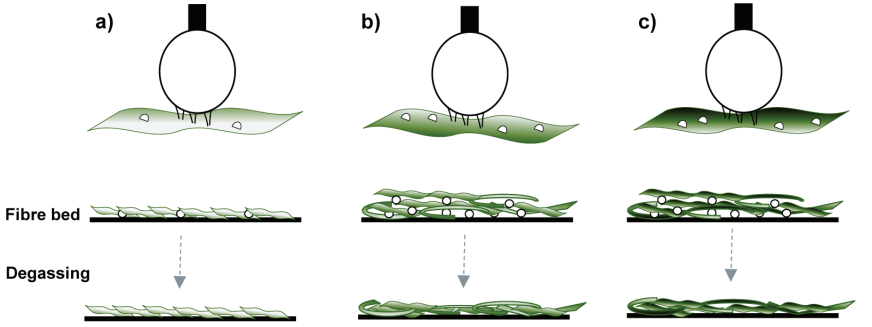

Viscose (0% lignin)
- Smooth surface, pure cellulose, low weight
- High attachment probability
- Attachment remains after degassing
- Sensitive to SDS addition

→ Fibre entanglement low in the fibre bed
→ Amphiphilicity may contribute to bubble-fibre interaction

Birch kraft (<5% lignin)
- Rough surface, mainly cellulose
- Low attachment probability
- Attachment decreases after degassing

→ Attachment via bubble-nanobubble and bubble-cellulose interaction
→ Fibre bed densifies after degassing and fibre entanglement increases, hindering the attachment probability

CTMP (30% lignin)
- Rough surface, high lignin content
- Moderate attachment probability
- Attachment increases after degassing

→ Attachment via bubble-lignin and bubble-cellulose interaction
→ Fibre bed densifies after degassing but high lignin-containing fibres have low entanglement

Figure 5. Mechanisms of bubble-fibre interaction with (a) viscose (b) birch and (c) CTMP, and the effect of degassing on a fibre bed.

Indeed, the degassing decreased the attachment with birch and pine kraft. However, with CTMP and viscose fibres, the attachment probability increased. It is possible that the removal of air actually densified the fibre bed, making the fibres even harder to be detached (Figure 5). Moreover, for CTMP with high lignin content, it is possible that the surface nanobubbles cause adhesion between the fibres in the bed. Removal of the surface nanobubbles thus decreases the fibre-fibre interaction and increases the CTMP attachment to the bubble (Figure 5).

In the case of light viscose fibres, the possible explanation for the high attachment probability could arise from the amphiphilic character of cellulose, straight fibre morphology and low fibre-fibre interaction and entanglement in the fibre bed. The captive bubble studies did not show any adhesion between pure cellulose and air bubble, but this system does not measure the actual adhesion force. The cellulose amphiphilic nature could result in a small bubble adhesion, which cannot be observed with the method. Also, straight and smooth viscose fibres have low interaction and entanglement in the fibre bed. Thus, it is possible that even a small attraction between the straight viscose and the bubble causes the attachment. As the interaction is weak, the fibres are easily detached from the bubble, and an external force is needed to really attach fibres onto the bubbles. Moreover, in dynamic forming conditions, the adhesion would be too small to keep fibres attached to bubbles. Free-floating fibres did not attach to bubbles, but they did slide along the bubble surface while passing them. In addition, the sensitivity of viscose for the SDS addition also indicated that the force between a viscose fibre and bubbles was very weak (Figure 4.)

There is no pre-existing data about the actual force between bubbles and cellulose in liquid environment. However, bubble-silica systems are extensively studied with an atomic force microscope (AFM). The surface free energies of silica and cellulose are similar (around 60 mN/m), cellulose having a bit higher dispersive and lower polar component and a higher contact angle (silica $\theta < 5°$, cellulose $\theta = 25°$) [40]. The bubble behaviour with silica has been reported to be rather inconsistent. Englert et al. (2009) and Tabor et al. (2011) have shown that in ultrapure water, only a repulsive force between the bubble and the silica particle can be detected (upon approach and retraction). But in some studies, a small adhesion during bubble retraction from silica has been observed [51], [52], and even a bubble jumping to contact has been reported [53], [54]. The controversial results could indicate that even slight variations in the system could result in small adhesion also for a fully wetted hydrophilic surface after the double layer force has been exceeded.

Bubble-Fibre Interaction and Dry Material Properties

After single bubble experiments, thick nonwoven materials were foam formed using hydrophilic and hydrophobic viscose fibres, with a small amount of CNF as

the binder and with anionic (SDS) and non-ionic (Tween20) surfactants (Figure 1c) [38]. The idea was to test the effect of surface hydrophobicity, which had been the main factor for the interaction strength in the earlier model surface and fibre bed studies besides fibre morphology. Large differences in fibre distribution and strength properties were observed when changing the fibre surface energy, keeping the forming conditions constant. Structures made with hydrophilic fibres were more oriented in the machine direction (MD) compared to hydrophobic fibres with both surfactant types (Figure 6a). A strong orientation resulted in better in-plane compression strength but lower z-strength (Figure 6b). Using anionic SDS as a surfactant, a rather connected structure with high z-strength was obtained with hydrophobic fibres, whereas the hydrophilic fibres led to a layered weaker structure in the thickness direction. However, the combination of hydrophobic fibre and the non-ionic surfactant was an interesting exception, showing a uniform structure that altered the strength properties in both the in-plane and z direction.

As it was also shown in the fibre bed studies (Figure 3), SDS addition decreases the bubble-fibre interaction. In a foam forming process, the used SDS concentration is commonly in the range of 0.02–0.2 g/L. Here we showed that already 0.1 g/L of SDS can weaken the interaction significantly. In this case, the fibres can flow freely in the foam and have a tendency to orientate themselves in the machine direction. The higher hydrophobic content of the fibres enhances the bubble-fibre interaction and results in better fibre mixing in the foam. Moreover, the surfactant

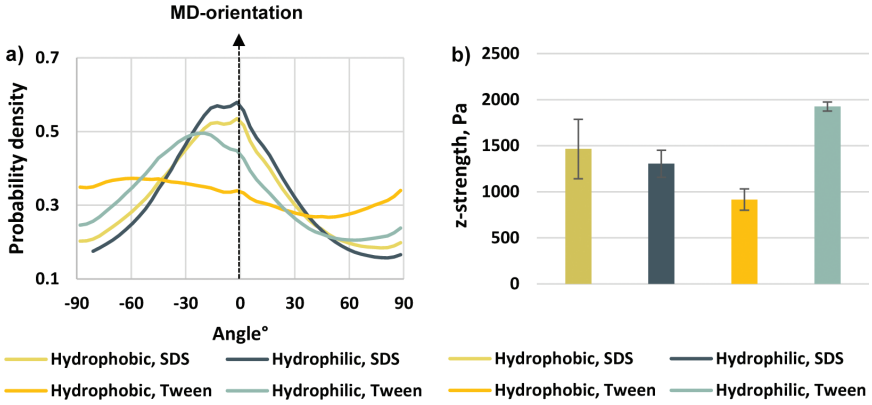

Figure 6. (a) The fibre orientation of the foam-formed structures in the x-y plane. The angle 0° corresponds to the x-direction (machine direction, MD), and angles ±90° correspond to the y-direction (cross direction, CD). (b) The z-directional tensile strength of the foam-formed structures.

type and concentration can affect the bubble adhesion, which is also reflected in the final material properties. The captive bubble studies with CNF films in Tween 20 solution showed an increase in the bubble interaction for the CNF film despite the very low surface tension (Figure 2). Also, the foam-formed cellulose structures prepared using Tween 20 were notably different when compared to structures formed with SDS. Thus, anionic and non-ionic surfactants both affected the bubble-fibre interaction but with different mechanisms [38]. As pointed out earlier, non-ionic surfactants with ethoxylated surfactant headgroups have been suggested to form bridges between surfactant micelles and cellulose fibrils [48]. Similar bridges are not expected to take place with anionic SDS.

CONCLUSIONS

Foam forming technology enables the production of sustainable materials with improved control of the microporous structure. The interaction of fibres with the foam carrier phase is an important tool for process control and product design. Our systematic research approach, where the complexity of the studied system is gradually increased, has clarified several important mechanisms of the bubble-fibre interaction. Single bubbles did not show any interaction with the smooth cellulose model surface but had a small adhesion to a rough CNF film. This effect was enhanced with electrolytes, whereas the addition of anionic surfactant (SDS) and degassing of the system decreased the interaction. Similar effects were observed for more complex fibre beds with some sensitivity to the fibre type and included surfactants. Based on the observations done with degassed CNF and fibre surfaces, it was suggested that the interaction between cellulose fibres and bubbles arises mainly from the hydrophobic content and entrapped nanobubbles at fibre surfaces. Direct imaging of nanobubbles on wet fibre surfaces using sophisticated imaging techniques would be needed to draw more decisive conclusions. Moreover, the bubble-fibre adhesion requires high enough liquid surface tension. The consequences were confirmed at a larger scale by foam forming bulky structures with hydrophobic and hydrophilic viscose fibres. The hydrophobicity of fibres affected their distribution and subsequent mechanical properties. Thus, the interaction mechanisms should be considered when developing industrial production processes and designing new materials.

ACKNOWLEDGEMENTS

This work was supported by the Academy of Finland (Grant No. 296851, Project ‘Surface interactions and rheology of aqueous cellulose-based foams’). We are

also grateful for the support from the FinnCERES Materials Bioeconomy Ecosystem. The authors would like to thank Katja Pettersson for the help with the AFM imaging of the CNF thin films and Tiina Pöhler and Mari Leino for CPD drying and SEM imaging of the fibres.

REFERENCES

[1] European Council, 'Directive (EU) 2019/904 of the European Parliament and of the Council of 5 June 2019 on the reduction of the impact of certain plastic products on the environment,' 2019.

[2] B. Radvan and A. P. J. Gatward, 'The formation of wet-laid webs by a foaming process,' *Tappi*, vol. 55, no. 5, p. 748–751, 1972.

[3] J. Lehmonen, P. Jetsu, K. Kinnunen and T. Hjelt, 'Potential of foam-laid forming technology in paper applications,' *Nord. Pulp Pap. Res. J.*, vol. 28, no. 3, pp. 392–398, 2013.

[4] T. Hjelt, J. A. Ketoja, H. Kiiskinen, A. I. Koponen and E. Pääkkönen, 'Foam forming of fiber products: a review,' in *Journal of Dispersion Science and Technology*, Taylor & Francis, 2020, pp. 1–37.

[5] A. Jäsberg, P. Selenius and A. Koponen, 'Experimental results on the flow rheology of fiber-laden aqueous foams,' *Colloids Surfaces A Physicochem. Eng. Asp.*, vol. 473, pp. 147–155, May 2015.

[6] A. M. Al-Qararah, T. Hjelt, A. Koponen, A. Harlin and J. A. Ketoja, 'Response of wet foam to fibre mixing,' *Colloids Surfaces A Physicochem. Eng. Asp.*, vol. 467, pp. 97–106, 2015.

[7] A. M. Al-Qararah et al., 'A unique microstructure of the fiber networks deposited from foam-fiber suspensions,' *Colloids Surfaces A Physicochem. Eng. Asp.*, vol. 482, no. January 2016, pp. 544–553, 2015.

[8] A. Madani et al., 'Ultra-lightweight paper foams: Processing and properties,' *Cellulose*, vol. 21, no. 3, pp. 2023–2031, 2014.

[9] T. Härkäsalmi, J. Lehmonen, J. Itälä, C. Peralta, S. Siljander and J. A. Ketoja, 'Design-driven integrated development of technical and perceptual qualities in foam-formed cellulose fibre materials,' *Cellulose*, vol. 24, no. 11, pp. 5053–5068, Nov. 2017.

[10] J. A. Ketoja, S. Paunonen, P. Jetsu and E. Pääkkönen, 'Compression strength mechanisms of low-density fibrous materials,' *Materials (Basel).*, vol. 12, no. 3, 2019.

[11] D. Whyte, B. Haffner, A. Tanaka and T. Hjelt, 'Interactions of fibres with simple arrangements of soap films,' *Colloids Surfaces A Physicochem. Eng. Asp.*, vol. 534, pp. 112–119, Dec. 2017.

[12] K. Schwinger and B. Dobias, 'The Influence of Calcium Ions of the Loss of Fibre in the Flotation Deinking Process,' in *2nd Research Forum on Recycling*, Montreal, Canada, 1991.

[13] H. Peng, G. R. Birkett and A. V. Nguyen, 'Progress on the Surface Nanobubble Story: What is in the bubble? Why does it exist?,' *Adv. Colloid Interface Sci.*, vol. 222, pp. 573–580, 2015.

[14] M. A. Hampton and A. V. Nguyen, 'Nanobubbles and the nanobubble bridging capillary force,' *Adv. Colloid Interface Sci.*, vol. 154, no. 1–2, pp. 30–55, 2010.
[15] X. Zhang, A. Kumar and P. J. Scales, 'Effects of solvency and interfacial nanobubbles on surface forces and bubble attachment at solid surfaces,' *Langmuir*, vol. 27, no. 6, pp. 2484–2491, 2011.
[16] N. Ishida, T. Inoue, M. Miyahara and K. Higashitani, 'Nano bubbles on a hydrophobic surface in water observed by tapping-mode atomic force microscopy,' *Langmuir*, vol.16, no. 16, pp. 6377–6380, 2000.
[17] R. Ajersch and M. Pelton, 'Mechanisms of pulp loss in flotation deinking,' *J. Pulp Pap. Sci.*, vol. 22, no. 9, pp. J338–J345, 1996.
[18] J. D. Redlinger-Pohn, M. Grabner, P. Zauner and S. Radl, 'Separation of cellulose fibres from pulp suspension by froth flotation fractionation,' *Sep. Purif. Technol.*, vol.169, pp. 304–313, 2016.
[19] Y. Deng and M. Abazer, 'True Flotation and Physical Entrapment: The Mechanisms of Fiber Loss in Flotation Deinking,' *Nord. Pulp Pap.*, vol. 13, no. 1, p. 4, 1998.
[20] Y. Deng, 'Effect of fibre surface chemistry on the fiber loss in flotation deinking,' *Tappi J.*, vol. 83, pp. 1–8, 2000.
[21] M. Preuss and H.-J. Butt, 'Direct Measurement of Particle–Bubble Interactions in Aqueous Electrolyte: Dependence on Surfactant,' *Langmuir*, vol. 14, no. 12, pp. 3164–3174, 1998.
[22] A. V. Nguyen, H. J. Schulze and J. Ralston, 'Elementary steps in particle—bubble attachment,' *Int. J. Miner. Process.*, vol. 51, no. 1–4, pp. 183–195, 1997.
[23] G. Wang, A. V. Nguyen, S. Mitra, J. B. Joshi, G. J. Jameson and G. M. Evans, 'A review of the mechanisms and models of bubble-particle detachment in froth flotation,' *Sep. Purif. Technol.*, vol. 170, pp. 155–172, 2016.
[24] H. Schubert, 'Nanobubbles, hydrophobic effect, heterocoagulation and hydrodynamics in flotation,' *Int. J. Miner. Process.*, vol. 78, no. 1, pp. 11–21, Dec. 2005.
[25] A. Sobhy and D. Tao, 'Nanobubble column flotation of fine coal particles and associated fundamentals,' *Int. J. Miner. Process.*, vol. 124, pp. 109–116, Nov. 2013.
[26] S.-T. Lou, Z.-Q. Ouyang and Y. Zhang, 'Nanobubbles on solid surface imaged by atomic force microscopy,' *J. Chem. Phys.*, vol. 18, p. 14706, 2000.
[27] L. Xie *e*t al., 'Interaction Mechanisms between Air Bubble and Molybdenite Surface: Impact of Solution Salinity and Polymer Adsorption,' *Langmuir*, vol. 33, no. 9, pp. 2353–2361, Mar. 2017.
[28] H. Peng, M. A. Hampton and A. V. Nguyen, 'Nanobubbles Do Not Sit Alone at the Solid–Liquid Interface,' *Langmuir*, vol. 29, no. 20, pp. 6123–6130, May 2013.
[29] J. D. Miller, Y. Hu, S. Veeramasuneni and Y. Lu, 'In-situ detection of butane gas at a hydrophobic silicon surface,' *Colloids Surfaces A Physicochem. Eng. Asp.*, vol. 154, no. 1–2, pp. 137–147, Aug. 1999.
[30] M. Li, L. Tonggu, X. Zhan, T. L. Mega and L. Wang, 'Cryo-EM Visualization of Nanobubbles in Aqueous Solutions,' *Langmuir*, vol. 32, no. 43, pp. 11111–11115, Nov. 2016.
[31] M. Switkes and J. W. Ruberti, 'Rapid cryofixation/freeze fracture for the study of nanobubbles at solid-liquid interfaces,' *Appl. Phys. Lett.*, vol. 84, no. 23, pp. 4759–4761, Jun. 2004.

[32] N. Hain, D. Wesner, S. I. Druzhinin and H. Schönherr, 'Surface Nanobubbles Studied by Time-Resolved Fluorescence Microscopy Methods Combined with AFM: The Impact of Surface Treatment on Nanobubble Nucleation,' *Langmuir*, vol. 32, no. 43, pp. 11155–11163, Nov. 2016.

[33] X. H. Zhang, 'Quartz crystal microbalance study of the interfacial nanobubbles,' *Phys. Chem. Chem. Phys.*, vol. 10, no. 45, p. 6842, Dec. 2008.

[34] R. Alén, *Basic chemistry of wood delignification*. Helsinki, Finland: Fapet Oy, 2000.

[35] K. Koljonen and P. Stenius, 'Surface characterisation of single fibres from mechanical pulps by contact angle measurements,' *Nord. Pulp Pap. Res. J.*, vol. 20, no. 1, pp. 107–113, 2005.

[36] K. Hodgson and J. Berg, 'Dynamic Wettability Properties of Single Wood Pulp Fibers and Their Relationship to Absorbency,' *Wood Fiber Sci.*, vol. 20, no. 1, pp. 3–17, 1988.

[37] M. F. Pucci, P.-J. Liotier and S. Drapier, 'Tensiometric method to reliably assess wetting properties of single fibers with resins: Validation on cellulosic reinforcements for composites,' *Colloids Surfaces A Physicochem. Eng. Asp.*, vol. 512, pp. 26–33, Jan. 2017.

[38] A. Ketola et al., 'Changing the structural and mechanical anisotropy of foam-formed cellulose materials by affecting bubble-fiber interaction with surfactant,' *ACS Appl. Polym. Mater.*, vol. submitted, 2022.

[39] S. Ahola, J. Salmi, L. S. Johansson, J. Laine and M. Österberg, 'Model films from native cellulose nanofibrils. Preparation, swelling, and surface interactions,' *Biomacromolecules*, vol. 9, no. 4, pp. 1273–1282, 2008.

[40] A. E. Ketola et al., 'Bubble Attachment to Cellulose and Silica Surfaces of Varied Surface Energies: Wetting Transition and Implications in Foam Forming,' *Langmuir*, vol. 36, no. 26, pp. 7296–7308, Jul. 2020.

[41] M. Aspiala, N. Schreithofer and R. Serna-Guerrero, 'Automated contact time apparatus and measurement procedure for bubble-particle interaction analysis,' *Miner. Eng.*, vol. 121, no. October 2017, pp. 77–82, 2018.

[42] D. I. Verrelli and B. Albijanic 'A comparison of methods for measuring the induction time for bubble–particle attachment,' *Miner. Eng.*, vol. 80, pp. 8–13, Sep. 2015.

[43] J. Vartiainen and T. Malm, 'Surface hydrophobization of CNF films by roll-to-roll HMDSO plasma deposition,' *J. Coatings Technol. Res.*, vol. 13, no. 6, pp. 1145–1149, 2016.

[44] A. W. Neumann and R. J. Good, 'Techniques of Measuring Contact Angles,' in *Surface and Colloid Science*, R. J. Good, Ed. New York, United States: Plenum Press, 1979, pp. 31–91.

[45] S. Mohammadi and T. Willers, 'Development of a measuring method for characterizing the surface of Pressure Sensitive Adhesives (PSA),' Hamburg, Germany, 2018.

[46] W. Xiang et al., 'How Cellulose Nanofibrils Affect Bulk, Surface, and Foam Properties of Anionic Surfactant Solutions,' *Biomacromolecules*, vol. 20, no. 12, pp. 4361–4369, Dec. 2019.

[47] I. M. Tucker, J. T. Petkov, J. Penfold and R. K. Thomas, 'Interaction of the Anionic Surfactant SDS with a Cellulose Thin Film and the Role of Electrolyte and Poyelectrolyte. 2 Hydrophilic Cellulose,' *Langmuir*, vol. 28, no. 27, pp. 10223–10229, Jul. 2012.

[48] N. Quennouz, S. M. Hashmi, H. S. Choi, J. W. Kim and C. O. Osuji, 'Rheology of cellulose nanofibrils in the presence of surfactants,' *Soft Matter*, vol. 12, no. 1, pp. 157–164, Dec. 2016.

[49] A. H. Englert, M. Krasowska, D. Fornasiero, J. Ralston and J. Rubio, 'Interaction force between an air bubble and a hydrophilic spherical particle in water, measured by the colloid probe technique,' *Int. J. Miner. Process.*, vol. 92, no. 3–4, pp. 121–127, Aug. 2009.

[50] R. F. Tabor, R. Manica, D. Y. C. Chan, F. Grieser and R. R. Dagastine, 'Repulsive Van der Waals forces in soft matter: Why bubbles do not stick to walls,' *Phys. Rev. Lett.*, vol. 106, no. 6, pp. 1–4, 2011.

[51] I. . Radtchenko, G. Papastavrou and M. Borkovec, 'Direct Force Measurements between Cellulose Surfaces and Colloidal Silica Particles,' *Biomacromolecules*, vol. 6, pp. 3057–3066, 2005.

[52] M. L. Fielden, R. A. Hayes and J. Ralston, 'Surface and Capillary Forces Affecting Air Bubble–Particle Interactions in Aqueous Electrolyte,' *Langmuir*, vol. 12, no. 15, pp. 3721–3727, 1996.

[53] W. A. Ducker, Z. Xu and J. N. Israelachvili, 'Measurements of Hydrophobic and DLVO Forces in Bubble–Surface Interactions in Aqueous Solutions,' *Langmuir*, vol. 10, no. 9, pp. 3279–3289, 1994.

[54] H.-J. Butt, 'A Technique for Measuring the Force between a Colloidal Particle in Water and a Bubble,' *J. Colloid Interface Sci.*, vol. 166, no. 1, pp. 109–117, Aug. 1994.

THE RELATION BETWEEN BUBBLE-FIBRE INTERACTION AND MATERIAL PROPERTIES IN FOAM FORMING

Annika Ketola[1], *Tuomo Hjelt*[1], *Timo Lappalainen*[1], *Heikki Pajari*[1], *Tekla Tammelin*[1], *Kristian Salminen*[1], *Koon-Yang Lee*[2], *Orlando Rojas*[3] *and Jukka A. Ketoja*[1]

[1] VTT Technical Research Centre of Finland Ltd, P.O. Box 1603, FI-40101 Jyväskylä, Finland
[2] Department of Aeronautics, Imperial College London, City and Guilds Building, SW7 2AZ, London, UK
[3] Bioproducts Institute, Departments of Chemical & Biological Engineering, Chemistry and Wood Science, The University of British Columbia, 2360 East Mall, Vancouver, BC V6T 1Z3, Canada

Steve Keller Miami University

Thank you for a clear explanation of how to do foam forming. You use surfactants to change the mechanism for forming, and my question goes to the very end and that is the effects of the surfactants on the mechanical properties. Not just the mechanical properties in the Z-direction like you demonstrated, but also other properties that could be affected by the SDS, and also maybe the hygroscopicity of the foams once they have been formed and how they behave in application. Do they absorb water differently because of the presence of the surfactant? So it seems that this is a two-part question; one is the effect of surfactants on the the mechanical properties and the second one is the potential aging of the solid foam under humid conditions.

Discussion

Annika Ketola

So, is your question about how do the remaining surfactants then affect the final material properties in the dry structure?

Steve Keller

That is correct.

Annika Ketola

If we make this very thin fibre structure so that we remove the water with vacuum, then the surfactant residue is quite small and they do not have a big role affecting, for example, the strength. However, if you compare to the thin water formed sheets, we can see that the foam formed structure is a bit bulkier, which again will be seen as a lower strength. With these much thicker structures where we do not remove the water and we have higher amounts of surfactant residues then they can have some role in the bonds between the fibres.

Steve Keller

Actually, the way it appears to me, the surfactant is acting at the surface. So there might be dissolved surfactant that washes away, but if you adsorb it on the surface, I would expect the interfibre behaviour to be different, and of course ultimately it is going to affect the way water or water vapour interacts with those fibres and in turn affect the strength properties.

Annika Ketola

That is true. Actually, with surfactants, we could imagine that the water goes easier into the structure because it has the lower surface tension, so through that it can affect absorption properties.

Steve Keller

Will that reduce strength of the material once it has been formed?

Annika Ketola

With these thick structures, we measured the z-directional strength and also the compression strength, but I cannot really compare to the water formed samples because we cannot do those without the foam.

Steve Keller

I guess what might be for further study would be to take the formed structure, increase the humidity and see if you lose insulating properties or mechanical properties because the uptake of water that can be attributed to the surfactants.

Annika Ketola

But of course, these are cellulose structures, they like to take water and humidity from the air. To prevent that, we would need to have some kind of other treatment for the fibres.

Natarajan Ramesh WestRock – Richmond VA

I was just wondering about the economics of the process. This is a batch process. Have you also worked on a continuous process? How do you make it more industrially applicable?

Annika Ketola

For the thick structures, we are working on how to make it continuous. It is not easy because the drying needs to be done in the oven, at the moment, but for thin structures we can do it continuously. So, if we want to make this kind of paper-like structures, then we can run it easily with the pilot machine.

Natarajan Ramesh

When bubbles are closed, the compression strength is very high and they will absorb shocks. So, what is the percentage of the closed cells in this particular form and does it fall under homogeneous nucleation or heterogeneous nucleation, and can you please comment on that?

Annika Ketola

I have not measured that.

Natarajan Ramesh

Okay. It is like open cell structure?

Annika Ketola

Yes, open cell structures.

Discussion

Natarajan Ramesh

That's the first question. The second one I was asking is about this nucleation aspect. Is it homogenous or heterogeneous and do you plan to add any nucleating agents down the road to change the dynamics of foam growth process?

Annika Ketola

I have not planned anything like that, but it is an interesting idea.

Jon Phipps FiberLean Technologies Ltd

Is it your assumption that the surface of viscose is pure cellulose? Do you have any way of verifying it, or whether there might be something else on the surface?

Annika Ketola

I have not checked or done any analysis for the viscose, but I am assuming that it is pure cellulose. Of course, when we have hydrophobic viscose, it's not pure cellulose, then we have this hydrophobisation on the surface.

Alexander Bismarck University of Vienna

I was wondering where the surfactant concentration was in relation to the CMC?

Annika Ketola

With SDS, it is lower but with the nonionic surfactant it is higher. With nonionic surfactants, to be able to make a good foam, we will need to add a lot of surfactant and we are usually operating at a much higher concentation than the CMC.

Alexander Bismarck

I was wondering with respect to the experiments where you attached the bubbles to pure regenerated cellulose or hydrophobic cellulose surfaces. You would expect that at least on the hydrophobic surface the surfactant will absorb. And if you increase surfactant concentration, it should to affect bubble adhesion, so bubbles should not attach anymore and with increasing surfactant concentration attach again.

Annika Ketola

We probably did not measure those high concentrations with SDS. We got to the point where it did not attach anymore, but we were not able to get to the point where it would attach again. You are probably referring to a double layer formation?

Alexander Bismarck

If the adsorbed surfactant forms a monolayer, then it should turn hydrophilic at lower concentration and should turn afterwards hydrophobic after formation of a bilayer again.

Annika Ketola

True, but we did not see that.

Alexander Bismarck

Anyhow it is not relevant to the foaming process.

Annika Ketola

That could be. It's a good point.